

# COUPLING THERMODYNAMIC CALCULATIONS AND SESSILE DROP METHOD TO UNDERSTAND THE PHYSICO-CHEMICAL REACTIVITY OF CERAMIC COMPOSITE MATERIALS AT HIGH TEMPERATURE

S.WERY and F. TEYSSANDIER

PROMES – CNRS UPR8521

Tecnosud – Rambla de la thermodynamique – 66100 Perpignan, France

sebastien.wery@univ-perp.fr

## ABSTRACT

Both fundamental and experimental works have been carried out to understand the thermochemical behaviour of borosilicate glasses according to several experimental parameters: temperature (400 to 1400°C), total pressure (0.1 to 30 atm), water vapour content in the gaseous phase (0 to 22%) and type of ceramic substrate (C, SiC and B<sub>4</sub>C). Using two softwares (Gemini2 and Thermocalc Classic), thermodynamic calculations were performed on ArBSiHO system. The purpose is to determine the experimental parameters that are responsible of a high rate of glass vaporisation and find out the influence of water vapour and silica on the rate of vaporization of B<sub>2</sub>O<sub>3(c)</sub>. Thermodynamic results were correlated with sessile drop experiments carried out in hot- and cold-wall reactors, as a function of T and amount of H<sub>2</sub>O in the atmosphere. Final contact angle and time necessary to reach equilibrium were both recorded for each system borosilicate glass / ceramic substrate.

## 1. INTRODUCTION

Ceramic matrix composites (CMC) such as C<sub>(f)</sub> / C<sub>(m)</sub> and SiC<sub>(f)</sub> / SiC<sub>(m)</sub>, are used in aerospace and aeronautic industries for the manufacturing of several parts such as nozzle, combustion chamber and exhaust cone [1, 2]. They replace, with success, superalloys in engine because of the combination of good thermo-physical properties (low density, refractoriness, chemical inertia, etc.) and good mechanical resistance. They permit to increase engine efficiency, reduce the size and the weight of the cooling system and decrease NO<sub>x</sub> emissions [3]. Thanks to the development of self healing matrix, the lifetime of CMC increases. It forms at low temperature (600°C) a liquid oxide (B<sub>2</sub>O<sub>3(l)</sub>) which fills in the cracks formed under thermo-mechanical stress. To protect the composite, the vitreous phase has to fulfill several criterions: (i) good wettability of the ceramic materials that are part of the CMC, (ii) low permeation to O<sub>2</sub>, (iii) physico-chemical compatibility with the ceramic materials and (iv) ability to form an oxide at low temperature [4].

In the present work, we focus on the behaviour of the sealing oxide (B<sub>2</sub>O<sub>3</sub>-SiO<sub>2</sub>) according to four parameters (temperature, pressure, atmosphere and type ceramic substrates). The purpose is to determine the reactivity of the sealing glass (infiltrations, volatilization, diffusion, etc.) as a function of the experimental conditions, associating experiments and thermodynamic calculations.

## 2. EXPERIMENTAL PROCEDURE

### 2.1. Thermodynamic calculation

Gemini2 and Thermocalc Classic software are used for thermodynamic calculations. Three hypotheses were assumed for the thermodynamic calculations: closed, isotherm and isobar system. We studied the influence of 3 parameters: (i) Temperature  $400 < T(^{\circ}\text{C}) < 1400$ ; (ii) Total pressure  $0.01 < P(\text{atm}) < 30$  atm; (iii) Composition of the gas phase:  $x \text{H}_2\text{O} + (1-x) \text{O}_2$ . MODDE software is used to display the surface response of  $\text{B}_2\text{O}_3(\text{g})$  vaporization.

### 2.2. Wetting law

On an ideal surface, the wetting of a liquid on a solid is characterized by the contact angle  $\theta$  defined by Young's equation [5]:

$$\cos \theta_Y = \frac{\sigma_{sg} \cdot \sigma_{sl}}{\sigma_{lg}} \quad (1)$$

$\sigma_{lg}$ ,  $\sigma_{sl}$  and  $\sigma_{sg}$  respectively correspond to liquid-gas, solid-liquid and solid-gas surface energies. Young's equation is related to wetting of ideal surfaces. However, several surface defects such as roughness [6], chemical heterogeneity [7], may be responsible for some departure from the ideal case.

### 2.3. Experimental set up

The sessile drop method was carried out both in hot- and cold-wall reactors. The hot wall set up is composed of a tubular kiln regulated by a thermocouple K (up to  $1100^{\circ}\text{C}$ ). The sample is located at the centre of the kiln and the drop is observed through quartz windows. The cold wall set up consists in a graphite susceptor coated by a silicon carbide layer and heated by induction. Temperature is regulated by a thermocouple S. (fig. 1). Both experimental set up are equipped with mass flow meters to control gas-phase composition and a numerical camera to measure the drop profile.

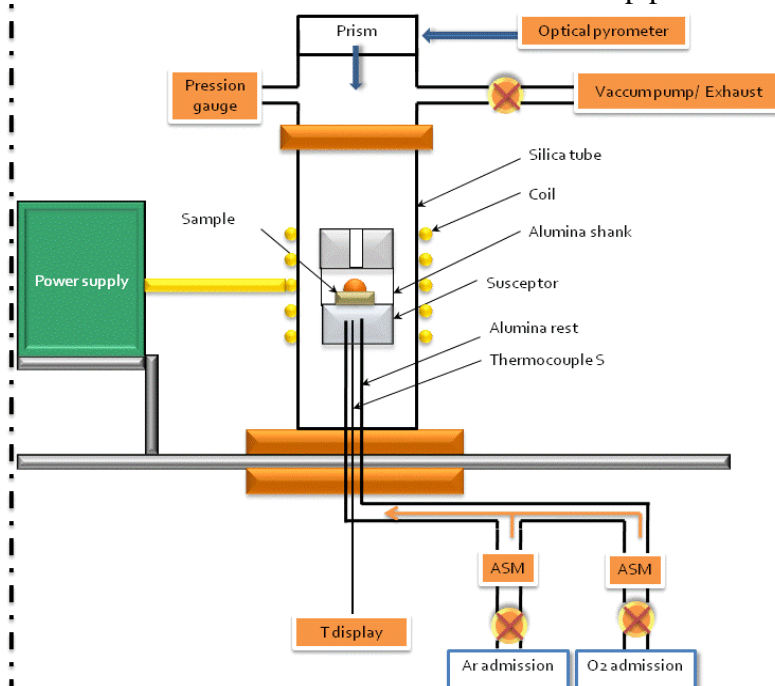


Figure 1: Cold wall set up

Both the drop contact angle ( $\theta \pm 2^\circ$ ) and the surface of contact between the drop and the substrate are measured during experiments using ImageJ software. Temperature ramp is equal to  $5^\circ\text{C}/\text{min}$  for the hot wall reactor and  $100^\circ\text{C}/\text{min}$  for the cold one.

## 2.4. Experimental procedure

Borosilicate glasses were prepared by fusion in a solar furnace:  $\text{B}_2\text{O}_3$  (s) and  $\text{SiO}_2$  (s) powders (Sigma Aldrich 99.99%) were melted at the focus of a solar concentrator (2kW, Odeillo, France) to obtain spherical drops. The mass of the drop must be small enough (around 80-100 mg) to avoid the influence of gravity [8]. Among all the materials that were experimentally tested (vitreous carbon, SiC and  $\text{B}_4\text{C}$ ) only the vitreous carbon substrates (bulk material Carbon Lorraine V25) were mechanically polished with diamond paste down to  $1\mu\text{m}$ . All other materials are thick coatings that were used as deposited. Their roughness was measured by AFM (NT-MDT, SEMA). All these materials were ultrasonically cleaned in ethanol before being introduced into the reactor.

The following parameters were used: total flow rate  $8\text{l}/\text{h}$  and a heating rate of  $5^\circ\text{C}/\text{min}$ . Two gas phase compositions were studied:  $0.78 \text{ Ar} + 0.22 \text{ O}_2$  or  $0.78 \text{ Ar} + 0.22 \text{ H}_2\text{O}$ . The duration of each experiment (up to 30h for some samples) was determined by the time required to reach equilibrium. At the end of each experiment, the sample was cooled down by conduction-convection process under reactive gas-phase. The morphological observations and chemical analyses were carried out by use of scanning electron microscopy (SEM, Hitachi S4500) coupled with energy dispersive spectroscopy (EDS, Noran-Vantage) or environmental scanning electron microscopy (ESEM, Philips XL30).

## 3. THERMODYNAMIC CALCULATIONS IN THE B-H-O-SI SYSTEM

The purpose of these calculations is to understand the influence of the operating conditions on the stability of  $\text{B}_2\text{O}_3$  (c). In a previous work, we have shown that  $\text{B}_2\text{O}_3$  reacts with water vapor to form  $\text{H}_x\text{B}_y\text{O}_z$  (g) species and that  $\text{HBO}_2$  (c) has a significant influence at low temperature by limiting its vaporisation [9].

Several calculations were carried for pure boron oxide and two typical compositions of borosilicate glasses:  $\text{B}_2\text{O}_3 = 1 \text{ mole}$  ;  $\text{B}_2\text{O}_3 = 0.75 \text{ mole} + \text{SiO}_2 = 0.25 \text{ mole}$  ;  $\text{B}_2\text{O}_3 = 0.25 \text{ mole} + \text{SiO}_2 = 0.75 \text{ mole}$ . Gas phase is composed of  $\text{Ar} + \text{O}_2 + \text{H}_2\text{O}$  ( $0.78/x/(1-x)$ ) so that  $x\text{O}_2 + (1-x)\text{H}_2\text{O} = 0.22 \text{ mole}$ ). The ratio of vaporized  $\text{B}_2\text{O}_3$ (c) is represented by an intensive parameter:

$$\% \text{B}_2\text{O}_3(\text{vaporized}) = \frac{(n_{\text{B}_2\text{O}_3(\text{s})}^{\text{initial}} - n_{\text{B}_2\text{O}_3(\text{s})}^{\text{final}})}{n_{\text{gas}}} \cdot 100 \quad (2)$$

Where  $n_{\text{B}_2\text{O}_3(\text{s})}$  (initial and final) are respectively the initial and equilibrium mole number of  $\text{B}_2\text{O}_3$ (s), and  $n_{\text{gas}}$  is the mole number of gaseous species at equilibrium.

For these calculations we used the thermodynamic model that we developed to describe the interactions between  $\text{B}_2\text{O}_3$  and  $\text{SiO}_2$  in borosilicate liquids. These interactions were adjusted to fit the  $\text{B}_2\text{O}_3$ - $\text{SiO}_2$  phase diagram (fig.2) experimentally determined by Rockett and al. [12].

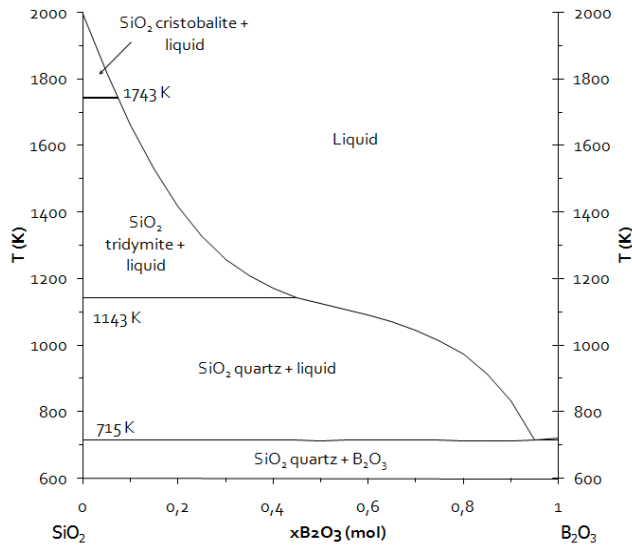
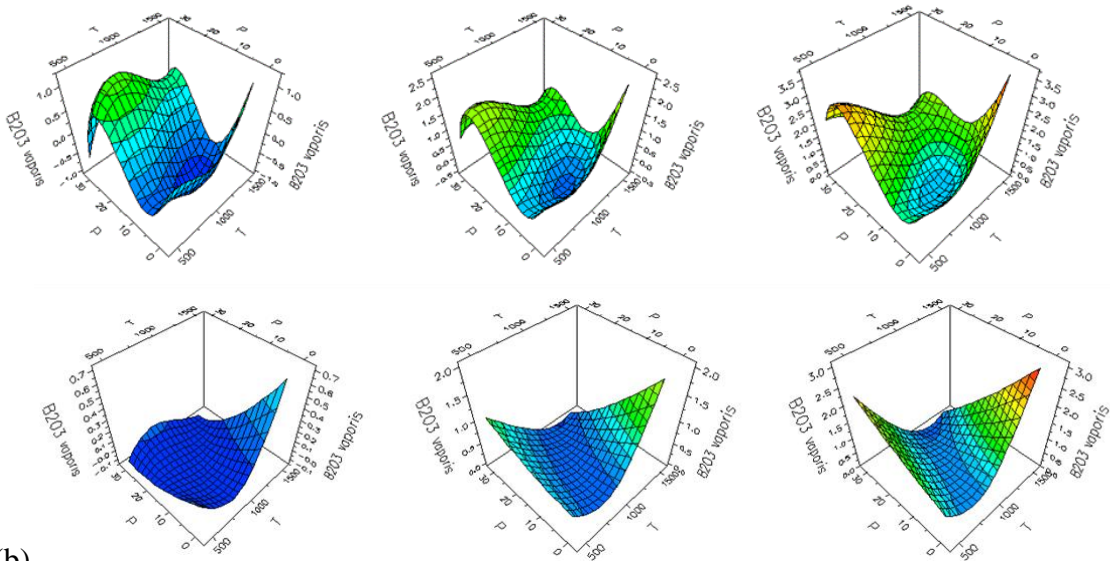


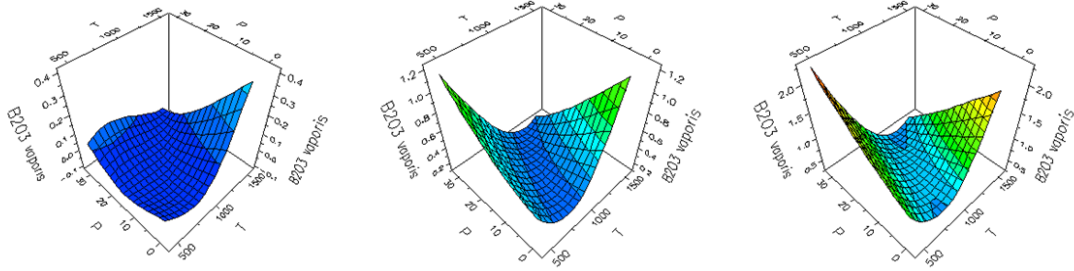
Figure 2 : Calculated  $B_2O_3$ - $SiO_2$  phases diagram

Looking at the various surfaces corresponding to the variations of the ratio of vaporized  $B_2O_3$ , one can observe the influence of  $H_2O$  and silica contents on borosilicate vaporization:  $H_2O$  enhances vaporization whereas silica content has the opposite effect (fig. 3). The sets of parameters corresponding to the highest  $B_2O_3$  (c) vaporization ratio are:  $P = 0.1$  atm,  $T = 1400^\circ C$ ,  $\%H_2O = 28\%$ , and  $P = 30$  atm,  $T = 800^\circ C$ ,  $\%H_2O = 28\%$ . Both domains correspond to the same preponderant gaseous species.

(a)



(b)



(c)

Figure 3 : Variation of the  $B_2O_3$  (c) vaporization ratio as a function of T, P and  $H_2O$  (g) content ((a) 100%  $B_2O_3$ , (b) 75%  $B_2O_3$ - $SiO_2$  and (b) 25%  $B_2O_3$ - $SiO_2$ ).

As already experimentally observed [13], the increased amount of Si-O-B bonds at high temperature when silica content increases tends to decrease the  $B_2O_3$  vaporisation.

#### 4. REACTIVITY BETWEEN BOROSILICATE GLASSES AND CERAMIC SUBSTRATES

The contact angle ( $\theta$ ) and the surface of the drop base (SDB), which is the interface between the drop and substrate, have been studied according to time and temperature. For all the curves related to the time dependence, time "0" corresponds to the beginning of the level temperature: the variations of  $\theta$  and SDB taking place during the temperature ramp are not displayed. The long times required to reach equilibrium are indicative of reactive wetting. Experiments under wet atmosphere have only been carried out in the hot wall reactor.

##### 4.1. Reactivity in $O_2$ atmosphere

The reactivity between liquid  $B_2O_3$  and the three substrates is temperature dependant: the contact angle decreases when the temperature increases. For  $T > 700^\circ C$ , whatever the couple glass / ceramic substrate, perfect wetting is observed. To understand  $\theta$  variation, one may consider not only the phenomenon of drop spreading over substrate surface, but also the substrate oxidation:

- The surface oxidation of carbon substrates induces the formation of porosities into which  $B_2O_3$  can infiltrate,
- An oxide film is formed at the surface of carbide substrates

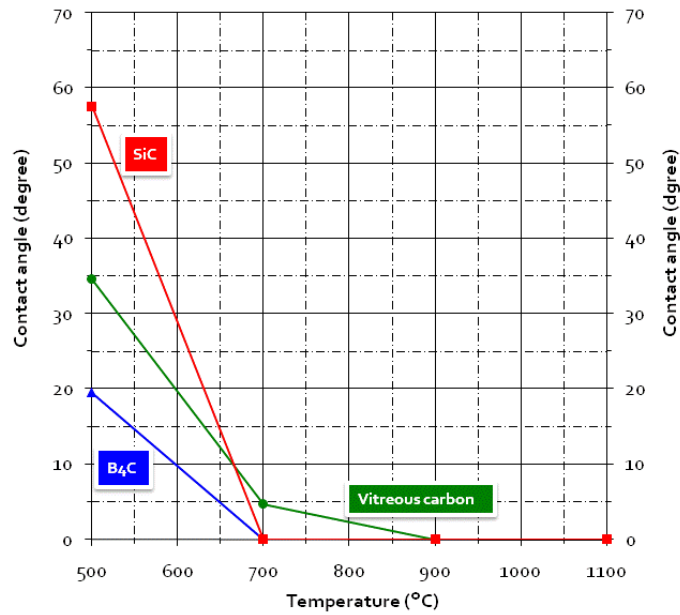


Figure 4: Variation of contact angle according to T and nature of the substrate under Ar + O<sub>2</sub> atmosphere in hot wall reactor.

In the case of carbon substrates, the oxidation that forms CO<sub>(g)</sub> and CO<sub>2(g)</sub> increases with temperature. At T > 800°C, the oxidation kinetics is so fast, that after 3h of thermal treatment, the substrate has completely disappeared. The porosities that result from carbon corrosion have significant influence on the spreading of the B<sub>2</sub>O<sub>3</sub> liquid. Three steps are observed: (i) growth of the drop base until a maximum surface of contact is reached, (ii) steady state where the drop base remains unchanged and (iii) shrinkage of the drop base.

Due to the rapid oxidation of carbon in oxidizing atmosphere above 800°C, we used the cold wall reactor that allows reaching quickly the level temperature, to study the variation of the contact angle up to 1100°C. The decrease of the contact angle when temperature increases above 800°C is conspicuous in fig.5. This phenomenon can be explained by the modification of the carbon surface morphology induced by corrosion: micro and macro porosities are responsible for enhanced roughness and presence of CO and CO<sub>2</sub> bubbles trapped below the B<sub>2</sub>O<sub>3</sub> drop. Both roughness (Wenzel model) and chemical heterogeneities (Cassie model) are responsible for the non wetting behavior in this case (fig. 6).

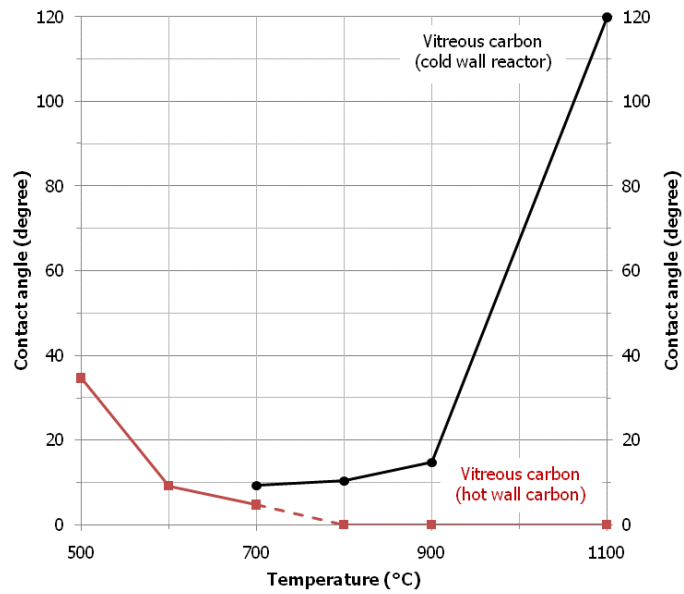


Figure 5: Variation of contact angle of  $B_2O_3$  on vitreous carbon as a function of temperature in Ar +  $O_2$  atmosphere.

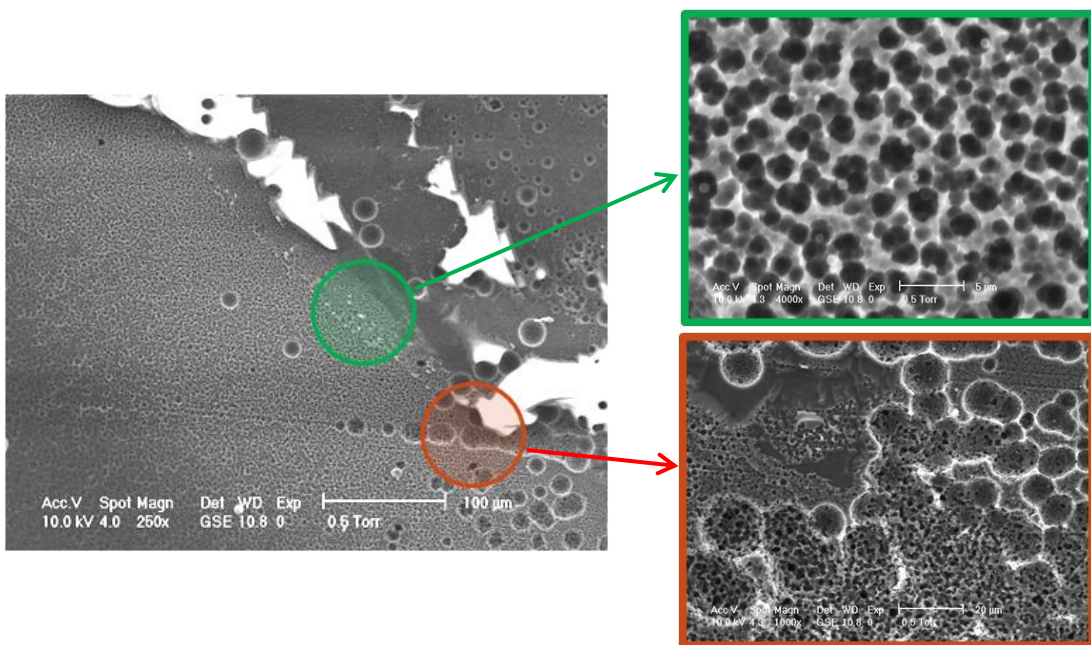


Figure 6: Surface morphology of a glass / carbon sample corroded at 1100°C.

These experiments underline the different behaviors of  $B_2O_3$  (l) on carbon according to temperature: below 700 – 800°C  $B_2O_3$  wets carbon and tends to infiltrate the porosities resulting from surface oxidation, protecting the surface from further oxidation. In

contrast at higher temperatures, the corrosion phenomena are so fast that the gas formation in the porosities tends to promote non wetting behavior, thus preventing any protection against oxidation.

In the case of carbides, the formation of an oxide layer at the surface provides a strikingly different picture. At  $T > 700^{\circ}\text{C}$ , the oxide formation at the carbide surface is fast and the drop spreads easily on a uniform oxide film. At lower temperatures, the film oxide is not uniform at the carbide surface and the drop participates to the formation of the oxide layer at the interface solid / liquid. High temperatures favor the formation of strong Si-O-B (SiC substrate) or B-O-B ( $\text{B}_4\text{C}$  substrate) bonds and  $\theta$  decreases rapidly. The drop tends to form a uniform film at the surface of the substrate.

The cold wall reactor allows in this case following the formation of the oxide film at the surface of the carbide substrate. The successive pictures reveal the formation of small drops that tend to merge as they grow (fig. 7)

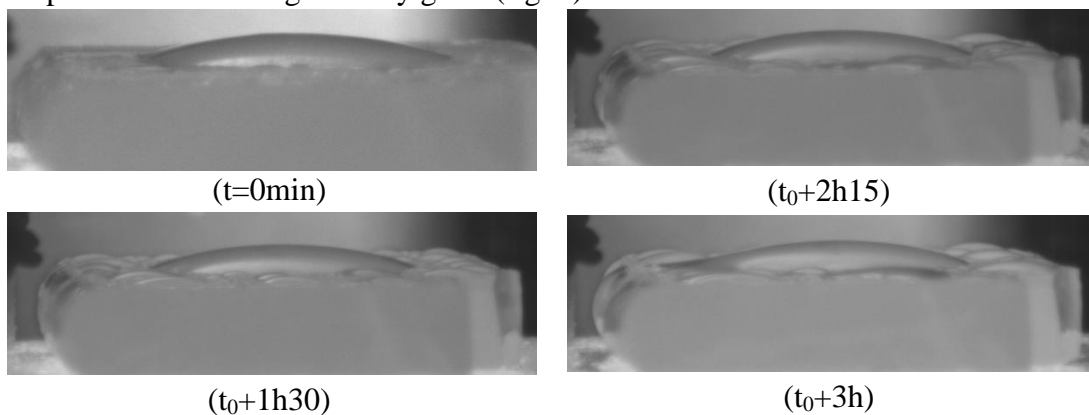


Figure 7: Behavior of  $\text{B}_2\text{O}_3 / \text{B}_4\text{C}$  system at  $900^{\circ}\text{C}$  in  $\text{Ar} + \text{O}_2$  in cold wall reactor.

#### 4.2. Reactivity in $\text{H}_2\text{O}$ atmosphere

In wet atmosphere, two domains are clearly observed as a function of temperature. non wetting at  $T < 700^{\circ}\text{C}$ , and perfect wetting above (fig. 8).

The lack of wetting observed at  $500^{\circ}\text{C}$  is due to the adsorption of water molecules on the reactive sites of ceramic substrates which prevents any reactivity between the drop and the substrate. At higher temperatures, the time required to reach equilibrium decreases with  $T$ . In the presence of water vapor, the key factor is the reaction of  $\text{H}_2\text{O}$  with  $\text{B}_2\text{O}_3$  to form  $\text{H}_x\text{B}_y\text{O}_z(\text{g})$  species. This phenomenon is particularly important above  $600^{\circ}\text{C}$  [14, 15, 16, 17].

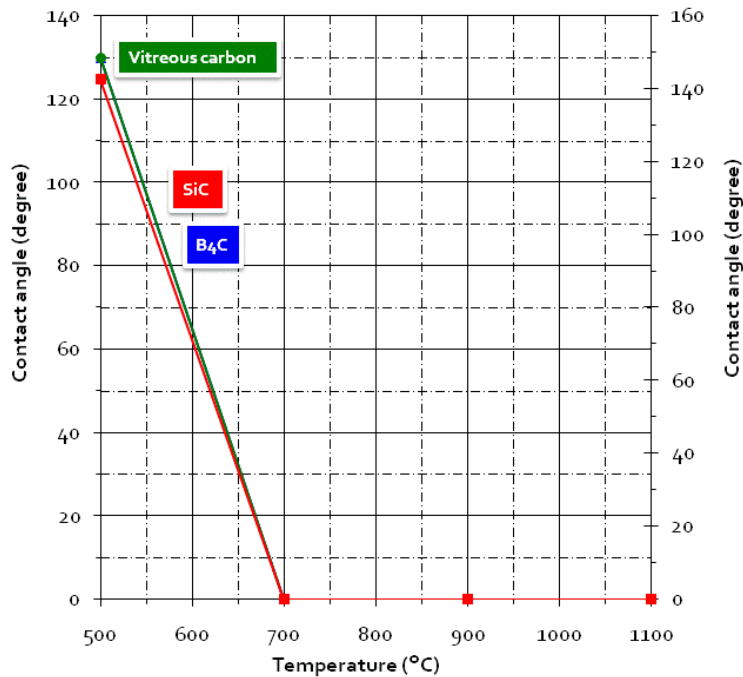


Figure 8: Variation of the contact angle as a function of T and nature of the substrate in Ar + H<sub>2</sub>O atmosphere.

Under wet atmosphere, the behaviour of each substrate is singular, thus we must distinguish the case of carbon, SiC and B<sub>4</sub>C. At a given temperature, corrosion of carbon is far less severe in the presence of water vapour than with oxygen and the reaction of B<sub>2</sub>O<sub>3</sub> with H<sub>2</sub>O is the main phenomenon. At temperature higher than 700°C, the experiment stops when all the B<sub>2</sub>O<sub>3</sub> has been consumed. The competition between the reactive wetting that tends to spread B<sub>2</sub>O<sub>3</sub> over the substrate and its reaction with H<sub>2</sub>O makes difficult the observation of the equilibrium state: perfect wetting may be confounded with the complete vaporization of B<sub>2</sub>O<sub>3</sub>. Nevertheless, the variation of the contact angle with time clearly converges towards perfect wetting above 700°C.

In the case of boron carbide substrates, SEM morphological observations underline the competition between oxidation and vaporisation phenomena. At high temperatures, the kinetics of vaporization of B<sub>2</sub>O<sub>3</sub> is faster than the oxidation of the B<sub>4</sub>C substrate: a strong corrosion of the carbide substrate is in this case observed (up to 30% for B<sub>4</sub>C at 900°C for example).

For SiC substrate, the reactivity is more complex: at T < 700°C, the kinetics of formation of SiO<sub>2</sub> is very low: B<sub>2</sub>O<sub>3</sub> vaporisation is the main process. At higher temperatures, B<sub>2</sub>O<sub>3</sub> reacts with SiO<sub>2</sub> that is formed by oxidation of the SiC surface, and a borosilicate film tends to protect the surface from further oxidation. Furthermore, the rate of B<sub>2</sub>O<sub>3</sub> vaporisation decreases because of the formation of Si-O-B bonds and substrate recession is smaller than with B<sub>4</sub>C substrate (about 15% at 1100°C). Thus, the competition between oxidation and vaporisation is more balanced than in B<sub>2</sub>O<sub>3</sub> / B<sub>4</sub>C system.

Finally, one can also observe the presence of small oxide crystals at the surface of the ceramic substrates. They have also been observed by Opila et al. and are nucleated by H<sub>2</sub>O.

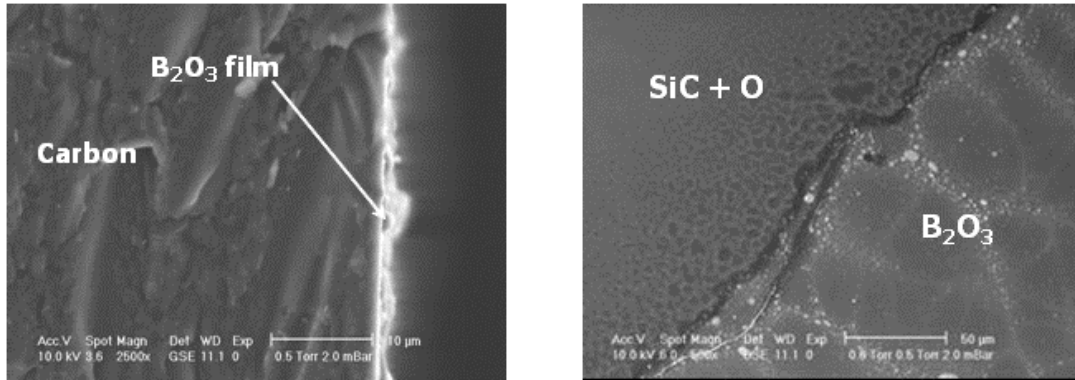


Figure 9: Morphological characterization of  $B_2O_3$  / carbon interface after thermal treatment at  $700^\circ C$  and top view of  $B_2O_3$  / SiC interface after thermal treatment at  $900^\circ C$ .

## CONCLUSION

The influence of temperature (400 to  $1400^\circ C$ ), total pressure (0.1-30 atm) and water vapor content (0 to 22%) on the vaporization of  $B_2O_3$  have been simulated in the B-H-O-Si by thermodynamic equilibrium calculations.

We underlined the strong influence of water vapour pressure on  $B_2O_3$  vaporization and determined the set of parameters that favours this phenomenon. Thermodynamic calculations with different  $B_2O_3$  /  $SiO_2$  ratio show the influence of  $SiO_2$  on  $B_2O_3$  vaporisation rate. Due to the formation of Si-O-B bonds, silica tends to reduce the vaporisation of the oxide at high temperature.

We investigated also the wetting behaviour of  $B_2O_3$  on carbon and carbide substrates by the sessile drop technique in  $O_2$  or  $H_2O$  atmosphere. Two experimental set up (a hot and cold wall reactor) have been designed to study the influence of temperature (500 to  $1100^\circ C$ ), water vapor content (0 to 22%) and nature of substrate. By running experiments in  $Ar + O_2$  and  $Ar + H_2O$  atmospheres, we have been able to distinguish between the influence of oxygen and water vapor on the behavior of  $B_2O_3$  / ceramic systems.

## ACKNOWLEDGEMENT

This work was funded by the joint research program "CPR DDV CMC" between Snecma Propulsion Solide (groupe Safran), DGA and CNRS.

## REFERENCES

- 1- R. NASLAIN, "Design, preparation and properties of non-oxide CMC for application in engines and nuclear reactors: an overview", *Composites Science and Technology*, 2004, n°64, p. 155-170.
- 2- S. SCHMIDT, S. BEYER, H. KNABE, H. IMMICH, R. MEISTRING and A. GESSLER, Advanced ceramic matrix composite materials for current and future propulsion technology application, *Acta Astronautica*, 2004, n°55, p. 409-420.

- 3- F. LAMOUREUX, S. BERTRAND, R. PAILLER, R. NASLAIN and M. CATALDI, Oxidation-resistant carbon-fiber-reinforced ceramic-matrix composites, *Composites Science and Technology*, 1999, n°59, p. 1073-1085.
- 4- R. NASLAIN, A. GUETTE, F. REBILLAT, R. PAILLER, F. LANGLAIS and X. BOURRAT, Boron-bearing species in ceramic matrix composites for long-term aerospace application, *Journal of Solid State Chemistry*, 2004, n°177, p. 449-456.
- 5- T. YOUNG, *Philos. Trans. R. Soc. (London)*, 1805, vol. 95, p. 65-87.
- 6- R.N. WENZEL, *Industrial and Engineering Chemistry*, 1936, vol. 28, n°8, p. 988.
- 7- A.B.D CASSIE and S. BAXTER, Wettability of Porous surfaces, *Trans. Faraday Soc.*, 1944, vol. 40, p. 546-551.
- 8- P.G. de GENNES, F. BROCHARD-WYART, D. QUERE, *Gouttes, bulles, perles et ondes*, 2002, Edition Belin, Collection Echelles.
- 9- S. WERY and F. TEYSSANDIER, Physico-chemical reactivity of ceramic composites materials at high temperature, International Meeting of the American Ceramic Society, Daytona, Florida, USA, 2007.
- 10- G. BARET, R. MADAR and C. BERNARD, Silica-based oxide systems, I. Experimental and Calculated Phase Equilibria in Silicon, Boron, Phosphorus, Germanium, and Arsenic Oxide Mixtures, *J. Electrochem. Soc.*, 1991, vol. 138, n°9, 2830-2835.
- 11- O. REDLICH and A.T. KISTER, Algebraic representation of thermodynamic properties and the classification of the solutions, *Industrial and Engineering Chemistry*, 1948, vol. 40, n°2, p. 345-348.
- 12- T.J. ROCKETT and W.R. FOSTER, Phase relations in the system boron oxide-silica, 1965, *Journal of the American Ceramic Society*, vol. 48, n°2, p. 75-79.
- 13- E. GARITTE, Thèse, Université de Bordeaux, 2007.
- 14- W. CHUPKA, M. INGRAM and R. PORTER, Mass Spectrometric Study of Gaseous Species in B-B<sub>2</sub>O<sub>3</sub> system, *Journal of Physics and Chemistry*, 1956, vol. 25, p. 498-501.
- 15- J.R SOULEN, P. STHAPITANONDA and J.L. MARGRAVE, Vaporization of Inorganic Substances: B<sub>2</sub>O<sub>3</sub>, TeO<sub>2</sub> and Mg<sub>3</sub>N<sub>2</sub>, *Journal of Physics and Chemistry*, 1955, vol. 59, p. 132-136.
- 16- N.S. JACOBSON, S. FARMER, A. MOORE and S. SAYIR, High Temperature Oxidation of Boron Nitride: I, Monolithic Boron Nitride, *Journal of the American Ceramic Society*, 1999, vol. 2, n°82, p. 393-398.
- 17- N.S. JACOBSON, G.N. MORSCHER, D.R. BRYANT and R.E. TESSLER, High-temperature Oxidation of Boron Nitride: II, Boron Nitride Layers in Composites, *Journal of the American Ceramic Society*, 1999, vol. 82, n°6, p. 1473-1482.